

Article

Stability Analysis in Determining Safety Drilling Fluid Pressure Windows in Ice Drilling Boreholes

Han Zhang ^{1,2,3}, Dongbin Pan ^{1,3}, Lianghao Zhai ^{1,3}, Ying Zhang ^{1,3} and Chen Chen ^{1,3,*}

¹ College of Construction Engineering, Jilin University, Changchun 130026, China; hanz16@mails.jlu.edu.cn (H.Z.); pandb16@mails.jlu.edu.cn (D.P.); dilh17@mails.jlu.edu.cn (L.Z.); yingzhang17@mails.jlu.edu.cn (Y.Z.)

² Polar Research Center, Jilin University, Changchun 130026, China

³ Key Laboratory of Drilling and Exploitation Technology in Complex Conditions, Ministry of Natural Resources, Changchun 130026, China

* Correspondence: chenchen@jlu.edu.cn; Tel.: +86-0431-88-502-678

Received: 3 November 2018; Accepted: 29 November 2018; Published: 3 December 2018



Abstract: Borehole stability analysis has been well studied in oil and gas exploration when drilling through rock formations. However, a related analysis of ice borehole stability has never been conducted. This paper proposes an innovative method for estimating the drilling fluid pressure window for safe and sustainable ice drilling, which has never been put forward before. First, stress concentration on a vertical ice borehole wall was calculated, based on the common elastic theory. Then, three failure criteria, the Mogi–Coulomb, teardrop, and Derradji-Aouat criteria, were used to predict the stability of the ice borehole for an unbroken borehole wall. At the same time, fracture mechanics were used to analyze the stable critical pressure for a fissured wall. Combining with examples, our discussion shows how factors like temperature, strain rate, ice fracture toughness, ice friction coefficient, and fracture/crack length affect the stability of the borehole wall. The results indicate that the three failure criteria have similar critical pressures for unbroken borehole stability and that a fissured borehole could significantly decrease the safety drilling fluid pressure window and reduce the stability of the borehole. The proposed method enriches the theory of borehole stability and allows drillers to adjust the drilling fluid density validly in ice drilling engineering, for potential energy exploration in polar regions.

Keywords: borehole stability; ice drilling; failure criteria; fracture mechanics; safety drilling fluid pressure window

1. Introduction

Maintaining the stability of a borehole is one of the most important tasks in oil and gas exploration [1]. When drilling into the earth's crust, using certain drilling fluids in the borehole wall is the most common way to balance the formation pressure [2]. Nonetheless, an inevitable stress concentration occurs around the borehole wall under this circumstance, and two borehole stability problems (borehole collapse and fracturing) occur if there is excessive stress concentration [3]. Borehole collapse could lead to stuck drilling tools, reaming operations, sidetracking, and even more serious drilling accidents. Meanwhile, borehole fracturing could result in the loss of drilling fluid and the enlargement of fractures on the borehole wall [4]. In actual drilling engineering, adjusting the drilling fluid pressure is an effective method to keep the borehole stable and is typically carried out by using a constitutive model to estimate the stresses around the borehole wall, coupled with a suitable failure criterion to obtain such critical drilling fluid pressures [4,5].

Numerous types of rocks failure criteria have been investigated by many researchers through triaxial compression tests [6–12]. On the basis of these proposed failure criteria, the problem of borehole

wall stability has been studied deeply. Aadnoy studied the effects of anisotropy on the stability of highly inclined boreholes when drilling into rock formations by developing an analytical solution [13]. Fuh applied this research method to the horizontal boreholes, which proved to be feasible [14]. Then, McLean analyzed the effect of the strength criteria and gave mud weight recommendations for actual drilling engineering [15]. Al-Ajmi compared the Mogi–Coulomb failure criteria with the Mohr–Coulomb and Druker–Prager failure criteria in a stability analysis of vertical boreholes and concluded that the Mogi–Coulomb law minimizes the conservative nature of drilling fluid pressure predictions [5,16]. As the research further developed, various failure criteria were studied and compared with each other for a more accurate drilling fluid weight prediction. At the same time, researchers also started to discuss the influence of laminated planes of weakness, pore pressure, and other factors on the borehole stability [3,17–20]. In general, the stability analysis of boreholes in rock formations has been well studied and applied in the actual oil and gas industry.

However, there are hardly any related studies of borehole stability in ice drilling. Set against this is the fact that many ice boreholes have displayed the phenomenon of borehole instability. For example, the drills were stuck several times at Vostok Station in a 5G borehole at a depth of 2250 m [21]. The same accident happened in the Dome F ice-core drilling project, Antarctica, in 1996 [22]. They were interpreted as a result of borehole collapse. As for ice borehole fracturing, in Dye-3 ice hole, drilled in Greenland between 1979 and 1981, a related survey showed a significant expansion or the presence of fractures at the bottom of the borehole [23]. In the season 2016–2017, the circulation of drilling fluid was suddenly lost at the Pirrit Hills ice drilling project, West Antarctica, near the ice–bedrock interface. A survey showed that fractures occurred in the borehole while increasing and reducing drilling fluid pressure [24]. Meanwhile, we observed the phenomenon of borehole collapse when we engaged in the Chinese first deep ice-core drilling project DK-1 at Dome A, Antarctica, during the working season of 2016–2017 (Figure 1). The ice drilling accidents described above require a reliable guidance for drillers when performing ice-core drilling engineering.

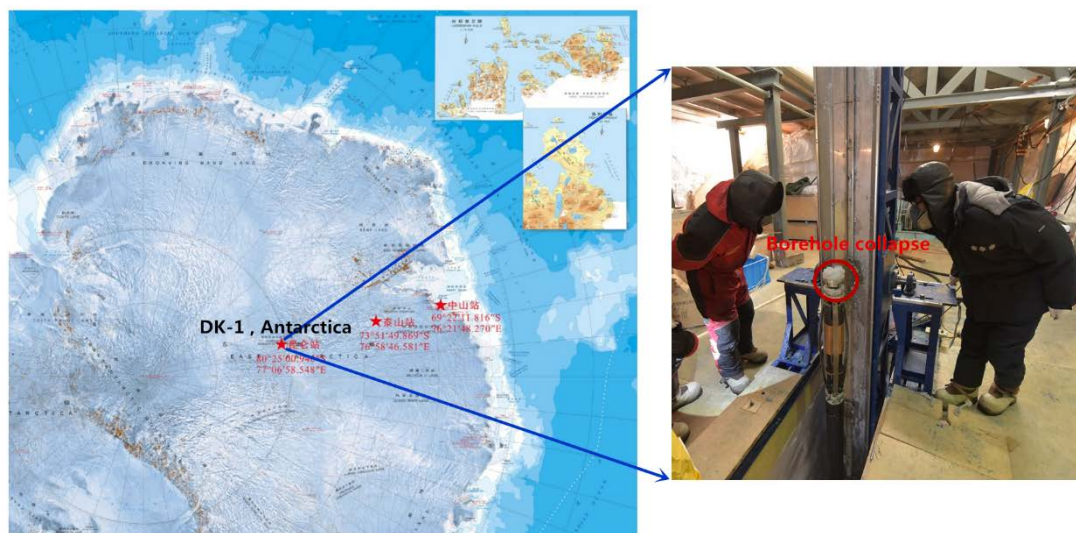


Figure 1. Location of the Chinese first deep ice-core drilling project DK-1 at Dome A, Antarctica, and the phenomenon of borehole collapse.

Recently, Chen studied hydraulic fracturing in ice boreholes and divided the borehole state into two situations: an unbroken borehole wall and a fissured borehole wall [24]. Based on this classification, we use different theoretical calculation methods to obtain the critical conditions for a stable ice borehole. For an unbroken borehole wall, following the same research method in rock formation boreholes, the proper failure criterion should first be taken into consideration for the brittle fracture of ice [4,5,15,16]. Nadreau [25] proposed a brittle failure criterion under triaxial tests with

plenty of fresh ice at a low confining pressure. This teardrop criterion considered the influence of hydrostatic pressure and met the tests result well. Then, Derradji-Aouat [26] described certain multi-surface brittle failure criteria of ice, according to the triaxial compression test data of fresh ice from experiments by Jones and Rist. These failure criteria considered the influence of temperature and strain rate and also proved to be effective in saline ice.

In this paper, we first introduce the teardrop and Derradji-Aouat failure criteria into an ice borehole and then innovatively compare the critical conditions for ice borehole stability by using these two ice failure criteria with the Mogi-Coulomb failure criteria (widely used in rock wellbore stability analysis) for an unbroken borehole wall. By considering the peculiarity of the different ice flows, ice temperature distributions, and behaviors under different strain rates in actual ice drilling, several points are discussed to show the influence of the horizontal stress differential, temperature, and strain rate on the critical pressure. As for a fissured borehole wall, the fracture mechanics method is introduced to determine the critical fracture instability condition on the borehole wall. Combining all circumstances, we try to figure out the mechanism of ice borehole stability, establishing the basis for adjusting the drilling fluid pressure and seeking for safe and efficient ice-core drilling in the future.

2. Theory of Stability Analysis in Ice Drilling Boreholes

The main purpose of drilling fluid is to maintain the stability of the borehole wall. However, a drilling fluid pressure that is too low could cause borehole collapse, while overpressure would cause borehole fracture. These two critical drilling fluid pressures determine the safety drilling fluid pressure range (safety drilling fluid pressure window) [4]. Before obtaining this pressure window, we should figure out two important points: the borehole state and the suitable criteria for instability.

Three different failure criteria were chosen to study each instance of critical drilling fluid pressure corresponding to borehole collapse and fracture for the unbroken wall, and fracture mechanics were accepted to analyze the stable critical pressure for the fissured wall. Combining every situation, we tried to find the most suitable pressure range for determining the safety drilling fluid pressure window in ice boreholes and provided the related theory to adjust the drilling fluid density for actual drilling.

2.1. Stress Distribution around the Borehole Wall

A large number of studies have been proposed to compute stresses around the borehole. Westergaard used an elasto-plastic model to obtain the stress distribution in his early works [27]. After that, various models have been put forward for the borehole stability problems, and among those published models, liner elastic analysis came to be the most commonly used, as it needs fewer parameters to be ensured [28–30]. According to the theory, the in situ stress, at a certain depth, generally consists of the vertical stress, σ_v , the maximum horizontal principal stress, σ_H , and the minimum horizontal principal stress, σ_h . Figure 2 shows the stress distribution around the borehole.

Through Kirsch's solution, when drilling a borehole, the stresses in a vertical borehole can be defined as [4,5]:

$$\sigma_r = \frac{1}{2}(\sigma_H - \sigma_h) \left(1 - \frac{R^2}{r^2}\right) + \frac{1}{2}(\sigma_H - \sigma_h) \left(1 - 4\frac{R^2}{r^2} + \frac{3R^4}{r^4}\right) \cos 2\theta + P_i \frac{R^2}{r^2}, \quad (1)$$

$$\sigma_\theta = \frac{1}{2}(\sigma_H - \sigma_h) \left(1 + \frac{R^2}{r^2}\right) - \frac{1}{2}(\sigma_H - \sigma_h) \left(1 + \frac{3R^4}{r^4}\right) \cos 2\theta - P_i \frac{R^2}{r^2}, \quad (2)$$

$$\sigma_z = \sigma_v - 2\nu(\sigma_H - \sigma_h) \cos 2\theta, \quad (3)$$

where σ_r , σ_θ , σ_z are the radial stress, hoop stress, and axial stress, respectively, at a distance r away from the borehole with the radius of R in polar coordinates. P_i is the drilling fluid pressure in the borehole, ν is Poisson's ratio of ice, and θ is measured clockwise from the σ_H direction.

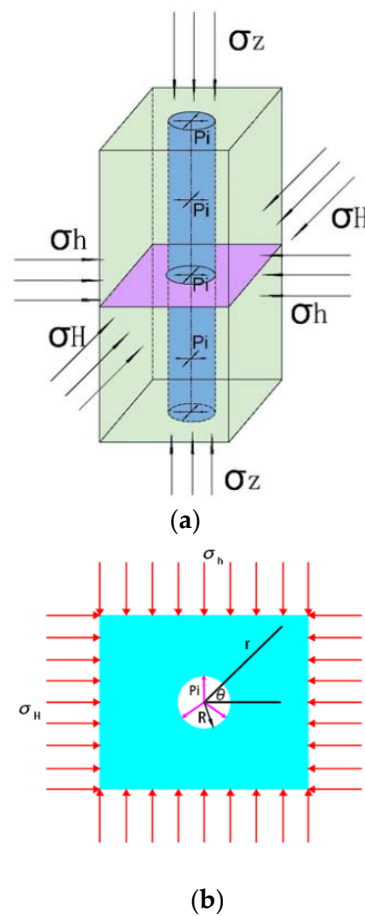


Figure 2. Stress distribution around the borehole. (a) 3D stress distribution at a certain depth; (b) stress distribution in the plane perpendicular to the axis of the ice borehole. (Chen, C., Polar Sci., in press, 2018)

At the borehole wall ($r = R$), the equations could change into:

$$\sigma_r = P_i, \quad (4)$$

$$\sigma_\theta = (\sigma_H + \sigma_h) - 2(\sigma_H - \sigma_h) \cos 2\theta - P_i, \quad (5)$$

$$\sigma_z = \sigma_v - 2v(\sigma_H - \sigma_h) \cos 2\theta, \quad (6)$$

According to the equations above, the hoop stress σ_θ and the axial stress σ_z are functions of the angle θ . The values reach a maximum at $\theta = \pm \frac{\pi}{2}$ and a minimum at $\theta = 0$ or π . We can conclude that a priori failure would occur at these points on the borehole [4].

From Equations (4) and (5), σ_r and σ_θ are functions of the drilling fluid pressure P_i . As we mentioned before, there are two instability problems that we should pay attention to: a drilling fluid pressure that is too low could cause borehole collapse, while overpressure would cause borehole fracture. When P_i decreases, σ_θ increases towards the ice compressive strength; therefore, the lower limit of the drilling fluid, P_c , corresponds to borehole collapse. Under this circumstance, σ_r should be less than σ_θ , and there are three permutations corresponding to borehole collapse: (1) $\sigma_\theta \geq \sigma_z \geq \sigma_r$, (2) $\sigma_\theta \geq \sigma_r \geq \sigma_z$, (3) $\sigma_z \geq \sigma_\theta \geq \sigma_r$. At the same time, borehole collapse would occur at $\theta = \pm \frac{\pi}{2}$, where the hoop stress has the largest value for the maximum collapse pressure. Three principle stresses are given by:

$$\sigma_r = P_i, \quad \sigma_\theta = A - P_i, \quad \sigma_z = B, \quad (7)$$

where:

$$A = 3\sigma_H - \sigma_h, \quad B = \sigma_v + 2v(\sigma_H - \sigma_h) \quad (8)$$

On the other hand, when P_i increases, σ_θ decreases towards the ice tensile strength; therefore, the upper limit of the drilling fluid, P_f , corresponds to the borehole fracture. Under this circumstance, σ_r should be larger than σ_θ , and there are three permutations corresponding to borehole fracturing: (1) $\sigma_r \geq \sigma_z \geq \sigma_\theta$, (2) $\sigma_z \geq \sigma_r \geq \sigma_\theta$, and (3) $\sigma_r \geq \sigma_\theta \geq \sigma_z$. At the same time, borehole fracturing would occur at $\theta = 0$ or π , where the hoop stress has the smallest value for the minimum fracturing pressure. Three principle stresses are given by:

$$\sigma_r = P_i, \sigma_\theta = D - P_i, \sigma_z = E, \quad (9)$$

where:

$$D = 3\sigma_h - \sigma_H, E = \sigma_v - 2\nu(\sigma_H - \sigma_h) \quad (10)$$

2.2. Stability Analysis for an Unbroken Ice Borehole Wall

2.2.1. The Mogi–Coulomb Criterion

The Mogi–Coulomb failure criterion is based on triaxial test data and it is widely used in different engineering applications. Several study results showed that the Mogi–Coulomb failure criterion is more precise than the Mohr–Coulomb one when calculating the borehole stability [5,16]. The criterion can be expressed as:

$$\tau_{oct} = a + b\sigma_{m,2}, \quad (11)$$

$$\tau_{oct} = \frac{1}{3}\sqrt{(\sigma_1 - \sigma_3)^2 + (\sigma_1 - \sigma_2)^2 + (\sigma_2 - \sigma_3)^2}, \quad (12)$$

$$\sigma_{m,2} = \frac{\sigma_1 + \sigma_3}{2}, \quad (13)$$

$$a = \frac{2\sqrt{2}}{3}S_0\cos\phi, b = \frac{2\sqrt{2}}{3}\sin\phi, \quad (14)$$

where S_0 and ϕ are, respectively, the cohesion and the internal friction angle of ice.

Based on the Mogi–Coulomb failure criterion above, we studied the borehole fracturing first; taking the most common situation, $\sigma_r \geq \sigma_z \geq \sigma_\theta$, for example, to study critical condition for borehole stability, it is:

$$\sigma_1 = \sigma_r = P_f; \sigma_2 = \sigma_z = E; \sigma_3 = \sigma_\theta = D - P_f, \quad (15)$$

Taking Equation (15) into the Mogi–Coulomb failure criterion:

$$\frac{1}{3}\sqrt{(P_f - (D - P_f))^2 + (P_f - E)^2 + (E - (D - P_f))^2} = a + b\frac{D}{2}, \quad (16)$$

By solving Equation (16), we could obtain the critical drilling fluid pressure P_f for borehole fracturing in this condition. Two other circumstances could also be calculated by using the same method, and Table 1 gives all of the equations of fracturing pressure.

When considering the borehole collapse, taking the most common situation, $\sigma_\theta \geq \sigma_z \geq \sigma_r$, for example, to study the critical condition for borehole stability, it is:

$$\sigma_1 = \sigma_\theta = A - P_c; \sigma_2 = \sigma_z = B; \sigma_3 = \sigma_r = P_c, \quad (17)$$

Taking Equation (17) into the Mogi–Coulomb failure criterion and using the same calculation method, Table 2 gives all of the equations of borehole collapse pressure.

Table 1. Mogi–Coulomb criterion for the determination of the fracturing pressure in an ice borehole.

Circumstances	$\sigma_1 \geq \sigma_2 \geq \sigma_3$	Borehole Fracturing Pressure
1	$\sigma_r \geq \sigma_z \geq \sigma_\theta$	$\frac{D}{2} + \frac{\sqrt{D^2 - 4Z_1}}{2}$
2	$\sigma_z \geq \sigma_r \geq \sigma_\theta$	$\frac{X_1}{2} + \frac{\sqrt{X_1^2 - 4Y_1}}{2}$
3	$\sigma_r \geq \sigma_\theta \geq \sigma_z$	$\frac{X_2}{2} + \frac{\sqrt{X_2^2 - 4Y_2}}{2}$

where: $D = 3\sigma_h - \sigma_H, E = \sigma_v - 2v(\sigma_H - \sigma_h)$

$$Z_1 = \frac{(D+E)^2}{3} - DE - \frac{3a^2 + 3abD + 0.75b^2D^2}{2}$$

$$X_1 = \frac{6D - 9ab - 4.5b^2(D+E)}{6 - 2.25b^2}$$

$$Y_1 = \frac{(2 - 2.25b^2)(D+E)^2 - 6DE - 9a^2 - 9ab(D+E)}{6 - 2.25b^2}$$

$$X_2 = \frac{6D + 9ab + 4.5Eb^2}{6 - 2.25b^2}$$

$$Y_2 = \frac{2(D+E)^2 - 6DE - 9a^2 - 9abE - 2.25(bE)^2}{6 - 2.25b^2}$$

Table 2. Mogi–Coulomb criterion for the determination of the collapse pressure in an ice borehole.

Circumstances	$\sigma_1 \geq \sigma_2 \geq \sigma_3$	Borehole Collapse Pressure
1	$\sigma_\theta \geq \sigma_z \geq \sigma_r$	$\frac{A}{2} - \frac{\sqrt{A^2 - 4Z_2}}{2}$
2	$\sigma_\theta \geq \sigma_r \geq \sigma_z$	$\frac{X_3}{2} - \frac{\sqrt{X_3^2 - 4Y_3}}{2}$
3	$\sigma_z \geq \sigma_\theta \geq \sigma_r$	$\frac{X_4}{2} - \frac{\sqrt{X_4^2 - 4Y_4}}{2}$

where: $A = 3\sigma_H - \sigma_h, B = \sigma_v + 2v(\sigma_H - \sigma_h)$

$$Z_2 = \frac{(A+B)^2}{3} - AB - \frac{3a^2 + 3abA + 0.75b^2A^2}{2}$$

$$X_3 = \frac{6A - 9ab - 4.5b^2(A+B)}{6 - 2.25b^2}$$

$$Y_3 = \frac{(2 - 2.25b^2)(A+B)^2 - 6AB - 9a^2 - 9ab(A+B)}{6 - 2.25b^2}$$

$$X_4 = \frac{6A + 9ab + 4.5Bb^2}{6 - 2.25b^2}$$

$$Y_4 = \frac{2(A+B)^2 - 6AB - 9a^2 - 9abB - 2.25(bB)^2}{6 - 2.25b^2}$$

2.2.2. The Teardrop Criterion

Nadreau J.P. concluded a special failure criterion for freshwater ice at low confining pressures [25]. The failure criterion considers the influence of changes in the ice physical properties and hydrostatic pressure; it is defined as:

$$q = \frac{3\sqrt{2}}{2} a_0 (b_0 - p) \left[1 + \frac{p - b_0}{b_0 - \sigma_t} \right]^{0.5}, \tag{18}$$

$$q = \sqrt{\frac{1}{2} ((\sigma_1 - \sigma_3)^2 + (\sigma_1 - \sigma_2)^2 + (\sigma_2 - \sigma_3)^2)}, \tag{19}$$

$$p = \frac{1}{3} (\sigma_1 + \sigma_3 + \sigma_3), \tag{20}$$

where q is the deviatoric stress, p is the hydrostatic pressure, a_0 is the parameter related to the pressure curve, for which some research suggests a constant value of about 0.1, b_0 is the ice phase transition pressure at a certain temperature, and σ_t is the ice tensile strength. This failure criterion has a good adaptability in both freshwater ice and brine polycrystalline ice.

Similarly, following the calculation process of the Mogi–Coulomb failure criterion, taking $\sigma_r \geq \sigma_z \geq \sigma_\theta$ as an example to study the critical fracturing pressure, Equation (15) is put into Equations (18)–(20), giving:

$$P_f^2 - DP_f + 3p^2 - 1.5a_0^2 (b_0 - p)^2 \left(1 + \frac{p - b_0}{b_0 - \sigma_t} \right) - DE = 0, \tag{21}$$

By solving this equation, the critical drilling fluid pressure P_f for borehole fracturing using the teardrop criterion could be obtained.

Using the same method, Tables 3 and 4 list all results on borehole collapse and fracturing pressure. Compared with the Mogi–Coulomb criterion, the teardrop criterion considers the influence of temperature, which is a vital parameter in ice boreholes. The ice phase transition pressure and tensile strength would be quite different at different temperatures, and the detailed parameter values are discussed in Section 3.

Table 3. Teardrop criterion for the determination of the fracturing pressure in an ice borehole.

Circumstances	$\sigma_1 \geq \sigma_2 \geq \sigma_3$	Borehole Fracturing Pressure
1	$\sigma_r \geq \sigma_z \geq \sigma_\theta$	$\frac{D}{2} + \frac{\sqrt{D^2 - 4Z_{TF}}}{2}$
2	$\sigma_z \geq \sigma_r \geq \sigma_\theta$	
3	$\sigma_r \geq \sigma_\theta \geq \sigma_z$	

where: $D = 3\sigma_h - \sigma_H$, $E = \sigma_v - 2v(\sigma_H - \sigma_h)$
 $p = \frac{D+E}{3}$
 $Z_{TF} = 3p^2 - 1.5a_0^2(b_0 - p)^2 \left(1 + \frac{p-b_0}{b_0-\sigma_t}\right) - DE$

Table 4. Teardrop criterion for the determination of the collapse pressure in an ice borehole.

Circumstances	$\sigma_1 \geq \sigma_2 \geq \sigma_3$	Borehole Collapse Pressure
1	$\sigma_\theta \geq \sigma_z \geq \sigma_r$	$\frac{A}{2} - \frac{\sqrt{A^2 - 4Z_{TC}}}{2}$
2	$\sigma_\theta \geq \sigma_r \geq \sigma_z$	
3	$\sigma_z \geq \sigma_\theta \geq \sigma_r$	

where: $A = 3\sigma_H - \sigma_h$, $B = \sigma_v + 2v(\sigma_H - \sigma_h)$
 $p = \frac{A+B}{3}$
 $Z_{TC} = 3p^2 - 1.5a_0^2(b_0 - p)^2 \left(1 + \frac{p-b_0}{b_0-\sigma_t}\right) - AB$

2.2.3. The Derradji-Aouat Criterion

Derradji-Aouat first proposed a multi-curved brittle failure criterion of fresh water ice by analyzing Jones and Rist’s triaxial compression test data on fresh water ice [26]; he had since applied this failure criterion to sea ice and has also achieved a good adaptability. The failure criterion can be defined as:

$$\left(\frac{q - \eta_s}{q_{s-max}}\right)^2 + \left(\frac{p - \lambda_s}{p_{sc}}\right)^2 = 1, \tag{22}$$

The yield surface of the criterion is the elliptic sphere; η_s and λ_s are the center coordinates of the ellipse in the data plane; q_{s-max} and p_{sc} respectively represent the short axis and the long axis of the ellipse. Also, we can obtain the value of q_{s-max} by the equations below:

$$q_{s-max} = [\dot{\epsilon}/\xi]^{1/n}, \tag{23}$$

$$\xi = 5 \times 10^{-6} \exp\left[-10.5 \times 10^{-3} \left(\frac{1}{T} - \frac{1}{273}\right)\right], \tag{24}$$

where $\dot{\epsilon}$ is the strain rate of loading, T is the Kelvin temperature, n is a parameter, and, according to the data fitting results of polycrystalline ice and columnar ice, $n = 2$. As for p_{sc} , the value can be obtained by:

$$p_{sc} + \lambda_s = b_0, \tag{25}$$

According to the phase diagram of water, we can obtain the value of b_0 ; the value of λ_s can be calculated through ice compressive tests data; the value of η_s just influences the position of the

yield surface and does not influence the size of the yield surface. In order to simplify the calculation, we assume $\eta_s = 0$.

Similarly, take $\sigma_r \geq \sigma_z \geq \sigma_\theta$, as an example to study the critical fracturing pressure. Equation (15) is put into Equations (19), (20), and (22), giving:

$$P_f^2 - DP_f - DE + \frac{1}{3}(D + E)^2 - \frac{q_{s-max}^2}{27p_{sc}^2} \left(6\lambda_s(D + E) - (D + E)^2 - 9(\lambda_s^2 - p_{sc}^2) \right) = 0, \quad (26)$$

By solving this equation, the critical drilling fluid pressure P_f for borehole fracturing using the Derradji-Aouat criterion could be obtained. Other critical pressures are shown in Tables 5 and 6.

Table 5. Derradji-Aouat criterion for the determination of the fracturing pressure in an ice borehole.

Circumstances	$\sigma_1 \geq \sigma_2 \geq \sigma_3$	Borehole Fracturing Pressure
1	$\sigma_r \geq \sigma_z \geq \sigma_\theta$	$\frac{D}{2} + \frac{\sqrt{D^2 - 4Z_{DAF}}}{2}$
2	$\sigma_z \geq \sigma_r \geq \sigma_\theta$	
3	$\sigma_r \geq \sigma_\theta \geq \sigma_z$	

where: $D = 3\sigma_h - \sigma_H$, $E = \sigma_v - 2v(\sigma_H - \sigma_h)$
 $q_{s-max} = [\dot{\epsilon}/\xi]^{1/n}$, $\xi = 5 \times 10^{-6} \exp[-10.5 \times 10^{-3}(\frac{1}{T} - \frac{1}{273})]$
 $p_{sc} + \lambda_s = b_0$
 $Z_{DAF} = \frac{1}{3}(D + E)^2 - DE - \frac{q_{s-max}^2}{27p_{sc}^2} (6\lambda_s(D + E) - (D + E)^2 - 9(\lambda_s^2 - p_{sc}^2))$

Table 6. Derradji-Aouat criterion for the determination of the collapse pressure in an ice borehole.

Circumstances	$\sigma_1 \geq \sigma_2 \geq \sigma_3$	Borehole Collapse Pressure
1	$\sigma_\theta \geq \sigma_z \geq \sigma_r$	$\frac{A}{2} - \frac{\sqrt{A^2 - 4Z_{DAC}}}{2}$
2	$\sigma_\theta \geq \sigma_r \geq \sigma_z$	
3	$\sigma_z \geq \sigma_\theta \geq \sigma_r$	

where: $A = 3\sigma_H - \sigma_h$, $B = \sigma_v + 2v(\sigma_H - \sigma_h)$
 $q_{s-max} = [\dot{\epsilon}/\xi]^{1/n}$, $\xi = 5 \times 10^{-6} \exp[-10.5 \times 10^{-3}(\frac{1}{T} - \frac{1}{273})]$
 $p_{sc} + \lambda_s = b_0$
 $Z_{DAC} = \frac{1}{3}(A + B)^2 - AB - \frac{q_{s-max}^2}{27p_{sc}^2} (6\lambda_s(A + B) - (A + B)^2 - 9(\lambda_s^2 - p_{sc}^2))$

Compared with the other two criteria above, this method mentions the strain rate of ice. We know that ice has different characteristics under different strain rates: at a low strain rate, it behaves with ductile deformation, while at a high strain rate, it behaves with brittle deformation. In general, the Derradji-Aouat criterion is more consistent with ice property changes and should be more accurate for determining the critical drilling fluid pressure in a borehole, but the downside is that the calculations require more parameters.

2.3. Stability Analysis for a Fissured Ice Borehole Wall

2.3.1. Instability Criterion

There are random cracks or fractures in a glacier, due to the interaction of various geological factors. When drilling through such an ice layer, the borehole wall itself is cracked. Such a fissured ice borehole wall contains some fractures that make the borehole wall incomplete; hence, we use the concept of the critical stress intensity factor (fracture toughness) in fracture mechanics to determine whether the borehole wall is unstable or not.

Taking a small fracture into consideration (Figure 3), we assume that it has an internal crack of length $2l_0$ and that the normal and shear stresses on the surface of the crack are [31–33]:

$$\sigma_{xx} = \frac{\sigma_1 + \sigma_3}{2} + \frac{\sigma_3 - \sigma_1}{2} \cos 2\varphi, \quad (27)$$

$$\sigma_{xy} = \frac{\sigma_3 - \sigma_1}{2} \sin 2\varphi, \quad (28)$$

where φ represents the angle between the crack and the direction of the maximum principal stress; σ_{xx} and σ_{xy} are the normal and shear stresses.

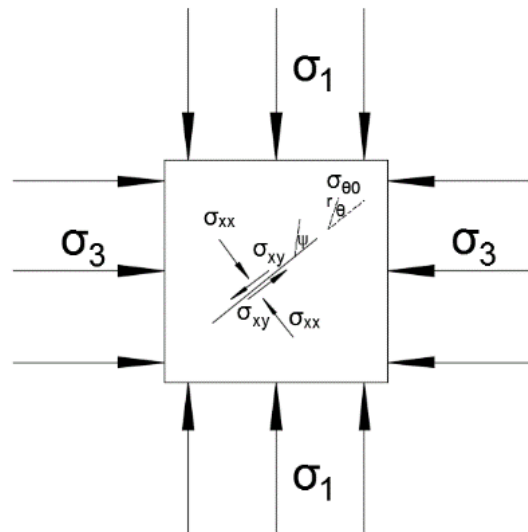


Figure 3. Force diagram around a small fracture.

The magnitude of the normal stress and the shear stress on the crack surface determines whether the crack grows or not. For the condition in which the crack is open, we divide the discussion into two parts:

1. Circumstance A:

When $\sigma_{xx} > 0$, the crack surface is in a state of tension. At this point, there is no friction on the crack surface, and the additional effect caused by the normal stress is not considered. We establish a polar coordinate system at the crack tip; the stress at the crack tip can be shown as:

$$\sigma_{\theta_0} = -\frac{3}{2} \left(\sigma_{xy} \frac{\sqrt{\pi l_0}}{\sqrt{2\pi r}} \sin \theta_0 \cos \frac{\theta_0}{2} + \sigma_{xx} \frac{\sqrt{\pi l_0}}{\sqrt{2\pi r}} \cos^3 \frac{\theta_0}{2} \right), \quad (29)$$

where θ_0 is the direction of crack growth.

Through fracture mechanics, the stress intensity factor at the crack tip is:

$$K_I = \lim_{r \rightarrow 0} \sqrt{2\pi r} \sigma_{\theta_0}, \quad (30)$$

Taking Equations (27)–(29) into Equation (30), we get:

$$K_I = -\frac{3}{2} \sqrt{\pi l_0} \cos \frac{\theta_0}{2} \left(\frac{\sigma_3 - \sigma_1}{2} \sin 2\varphi \sin \theta_0 + \left(\frac{\sigma_1 + \sigma_3}{2} + \frac{\sigma_3 - \sigma_1}{2} \cos 2\varphi \right) \cos^2 \frac{\theta_0}{2} \right), \quad (31)$$

In order to obtain the maximum value for K_I , the condition is:

$$\frac{\partial K_I}{\partial \theta_0} = 0, \quad \frac{\partial K_I}{\partial \varphi} = 0, \quad (32)$$

By solving Equation (32), we can get the critical K_I for crack extension:

$$K_I = \begin{cases} \sigma_3 \sqrt{\pi l_0}, & \varphi = 0 \\ \frac{\sigma_1 \sqrt{\pi l_0} (\Gamma - 1) \left[\frac{\Gamma + 1}{\Gamma - 1} + 0.5 \sin 4\varphi \tan 2\varphi \right]}{2(9 + \tan^2 2\varphi)^{1.5}}, & \varphi \neq 0 \end{cases}, \quad (33)$$

where: $\Gamma = \frac{\sigma_3}{\sigma_1}$.

2. Circumstance B

When $\sigma_{xx} < 0$, the crack surface is in a state of compression. At this point, we need to consider the additional force of friction under normal stress. The friction coefficient of the upper and lower surfaces of the crack is assumed to be μ_c ; when the crack starts to extend, the normal stress at the crack tip is also σ_{xx} , but the shear stress changes into:

$$\sigma'_{xy} = \sigma_{xy} + \mu_c \sigma_{xx}, \quad (34)$$

Similarly, the stress at the crack tip is:

$$\sigma_{\theta_0} = -\frac{3}{2} \left(\sigma'_{xy} \sin \theta_0 \cos \frac{\theta_0}{2} + \sigma_{xx} \frac{\sqrt{\pi l_0}}{\sqrt{2\pi r}} \cos^3 \frac{\theta_0}{2} \right), \quad (35)$$

Combining Equation (35) into Equation (30) and using the same method above to obtain the critical K_I , we obtain:

$$K_I = -\frac{\sigma_1 \sqrt{\pi l_0}}{\sqrt{3}} \left\{ (1 - \Gamma) (1 + \mu_c^2)^{0.5} - (1 + \Gamma) \mu_c \right\}, \quad (36)$$

Combining the circumstances A and B, the critical stress intensity factor for a borehole wall containing a crack of length $2l_0$ at the crack tip can be calculated:

$$K_I = K_a \sigma_1 \sqrt{\pi l_0}, \quad \begin{cases} K_a = -\frac{1}{\sqrt{3}} (1 - \Gamma) (1 + \mu_c^2)^{0.5} - (1 + \Gamma) \mu_c, & \sigma_{xx} \leq 0 \\ K_a = \frac{(\Gamma - 1) \left[\frac{\Gamma + 1}{\Gamma - 1} + 0.5 \sin 4\varphi \tan 2\varphi \right]}{2(9 + \tan^2 2\varphi)^{1.5}}, & \sigma_{xx} > 0 \end{cases}, \quad (37)$$

When this critical stress intensity factor exceeds the ice fracture toughness, the borehole wall becomes unstable.

2.3.2. Crack States on the Borehole Wall: Open or Closed?

In order to select the appropriate calculation formula of the critical stress intensity factor, we first needed to determine whether the crack was open or closed on the borehole wall [33]. We considered the following:

For borehole fracturing, take $\sigma_r \geq \sigma_z \geq \sigma_\theta$ for example; by considering positive for tension and negative for compression, take Equation (15) into (27):

$$\sigma_{xx} = -\frac{D(1 + \cos 2\varphi) - 2P_i \cos 2\varphi}{2} \ll -\frac{2D \cos 2\varphi - 2P_i \cos 2\varphi}{2} < 0, \quad (38)$$

Similarly, the state of the crack in the other two fracturing cases can be obtained, being, for both, $\sigma_{xx} < 0$.

For the borehole collapse, take $\sigma_\theta \geq \sigma_z \geq \sigma_r$ for example; take Equation (17) into (27):

$$\sigma_{xx} = -\left(\frac{A}{2} + \frac{2P_i - A}{2} \cos 2\varphi \right) \ll \frac{A}{2} \cos 2\varphi - \frac{2P_i + A}{2} \cos 2\varphi < 0, \quad (39)$$

The state of the crack in the other two collapse cases is also $\sigma_{xx} < 0$.

In summary, for both borehole fracturing and collapse, the state of the crack remains closed all the time. For the compression crack, the following critical relationship can be obtained:

$$K_{IC} = -\frac{\sigma_1 \sqrt{\pi l_0}}{\sqrt{3}} \left\{ (1 - \Gamma) (1 + \mu_c^2)^{0.5} - (1 + \Gamma) \mu_c \right\}, \tag{40}$$

where K_{IC} is the ice fracture toughness.

2.3.3. Critical Drilling Fluid Pressure

Similarly, taking $\sigma_r \geq \sigma_z \geq \sigma_\theta$ as an example, to study the critical fracturing pressure, combine Equation (15) into (40):

$$K_{IC} = \frac{P_f \sqrt{\pi l_0}}{\sqrt{3}} \left\{ \left(1 - \frac{D - P_f}{P_f} \right) (1 + \mu_c^2)^{0.5} - \left(1 + \frac{D - P_f}{P_f} \right) \mu_c \right\}, \tag{41}$$

By transforming Equation (41), the critical drilling fluid pressure for borehole fracturing is:

$$P_f = \frac{\frac{K_{IC} \sqrt{3}}{\sqrt{\pi l_0}} + D (\sqrt{1 + \mu_c^2} + \mu_c)}{2 \sqrt{1 + \mu_c^2}}, \tag{42}$$

Using the same calculation process, Table 7 gives all the critical drilling fluid pressures for borehole fracturing at different circumstances.

Table 7. Critical fracturing pressure for the fissured borehole wall.

Circumstances	$\sigma_1 \geq \sigma_2 \geq \sigma_3$	Borehole Fracturing Pressure
1	$\sigma_r \geq \sigma_z \geq \sigma_\theta$	$\frac{\frac{K_{IC} \sqrt{3}}{\sqrt{\pi l_0}} + D (\sqrt{1 + \mu_c^2} + \mu_c)}{2 \sqrt{1 + \mu_c^2}}$
2	$\sigma_z \geq \sigma_r \geq \sigma_\theta$	$D + \frac{\frac{K_{IC} \sqrt{3}}{\sqrt{\pi l_0}} - E (\sqrt{1 + \mu_c^2} - \mu_c)}{\sqrt{1 + \mu_c^2} + \mu_c}$
3	$\sigma_r \geq \sigma_\theta \geq \sigma_z$	$\frac{\frac{K_{IC} \sqrt{3}}{\sqrt{\pi l_0}} + E (\sqrt{1 + \mu_c^2} + \mu_c)}{\sqrt{1 + \mu_c^2} - \mu_c}$

where: $D = 3\sigma_h - \sigma_H$, $E = \sigma_v - 2\nu(\sigma_H - \sigma_h)$
 K_{IC} is the ice fracture toughness, μ_c is the friction coefficient between cracks, l_0 is the half-length of the crack.

Take $\sigma_\theta \geq \sigma_z \geq \sigma_r$, for example. To study the critical collapse pressure, combine Equation (17) into (40):

$$K_{IC} = \frac{(A - P_c) \sqrt{\pi l_0}}{\sqrt{3}} \left\{ \left(1 - \frac{P_c}{A - P_c} \right) (1 + \mu_c^2)^{0.5} - \left(1 + \frac{P_c}{A - P_c} \right) \mu_c \right\}, \tag{43}$$

By transforming Equation (43), the critical drilling fluid pressure for borehole collapse is:

$$P_c = \frac{A}{2} - \frac{A \mu_c + \frac{K_{IC} \sqrt{3}}{\sqrt{\pi l_0}}}{2 \sqrt{1 + \mu_c^2}}, \tag{44}$$

Using the same calculation process, Table 8 gives all the critical drilling fluid pressures for borehole collapse under different circumstances.

This part of the discussion is based on a fissured borehole wall zone, which involves the fracture toughness of ice, the size of the cracks, and the friction coefficient between the crack surfaces. The growth of the ice crystals is closely related to the temperature of the environment, the contents of the ions and impurities in the water, the long-term action of forces, etc. In different conditions,

the values of the parameters vary greatly; therefore, specific analysis should be made in combination with the actual situation before determining the borehole state.

Table 8. Critical collapse pressure for the fissured borehole wall.

Circumstances	$\sigma_1 \geq \sigma_2 \geq \sigma_3$	Borehole Collapse Pressure
1	$\sigma_\theta \geq \sigma_z \geq \sigma_r$	$\frac{A}{2} - \frac{A\mu_c + \frac{K_{IC}\sqrt{3}}{\sqrt{\pi}l_0}}{2\sqrt{1+\mu_c^2}}$
2	$\sigma_\theta \geq \sigma_r \geq \sigma_z$	$A - \frac{\frac{K_{IC}\sqrt{3}}{\sqrt{\pi}l_0} + B(\sqrt{1+\mu_c^2} + \mu_c)}{\sqrt{1+\mu_c^2} - \mu_c}$
3	$\sigma_z \geq \sigma_\theta \geq \sigma_r$	$\frac{-BK_{IC}\sqrt{3}}{\sqrt{\pi}l_0} + B(\sqrt{1+\mu_c^2} - \mu_c)$ $\sqrt{1+\mu_c^2} + \mu_c$

where: $A = 3\sigma_H - \sigma_h$, $B = \sigma_v + 2v(\sigma_H - \sigma_h)$
 K_{IC} is the ice fracture toughness, μ_c is the friction coefficient between cracks, l_0 is the half-length of the crack.

3. Results and Discussion

3.1. Critical Pressure for an Unbroken Ice Borehole Wall

3.1.1. Study A: Comparison of the Critical Borehole Fracturing and Collapse Pressure between the Three Failure Criteria

According to Hooke’s theory [34], the three principal stresses values are not very different in ice; we assume that a vertical borehole with a depth of 3000 m is drilled, the average overlying ice pressure gradient is $\sigma_v = 9$ kPa/m, the maximum and minimum horizontal principal stress gradients are $\sigma_H = 8.8$ kPa/m and $\sigma_h = 8.5$ kPa/m, and the temperature for the whole borehole is -10 °C for a simplified calculation. The density of the drilling fluid is taken as 923 kg/m³ (ignoring the influences of temperature and pressure) in the ice borehole to balance the ice pressure [21]. Other parameter values (Table 9) are accepted according to previous related studies [26,35]:

Table 9. Calculated value of each parameter in this study

Parameter	Value	Unit
Cohesion, S_0	1.204	MPa
Internal friction angle, ϕ	9.228	angle
Tensile strength, σ_t	0.81	MPa
Pressure phase transition, b_0	115	MPa
Strain rate, $\dot{\epsilon}$	10^{-3}	/s
Poisson’s ratio, ν	0.31	
Long axis of the ellipse, p_{sc}	55.0	MPa

Figure 4 gives us the critical borehole pressure changes with depth under the above assumed conditions. From the picture, we know that the borehole fracturing and collapse pressure calculated by the three failure criteria have little differences between each other, and we cannot obtain a certain critical pressure until ~600 m by using the Derradji-Aouat criterion (the equation has no real roots). These curves show that:

1. The drilling fluid pressure curve passes through the borehole stability area, which means that no collapse or fracturing occurs on the whole borehole wall;
2. When ice borehole depth is 600–1200 m, the window for the safety drilling fluid pressure with a stable borehole wall is the widest when calculated by the teardrop criterion and is the most conservative when calculated by the Derradji-Aouat criterion. With depth increases, the safety drilling fluid pressure window as calculated by the Derradji-Aouat criterion reaches

the maximum. Comparatively speaking, the Mogi–Coulomb criterion is the most stable failure criterion and is the most conservative in the deep range of 1200–1750 m.

In general, the critical pressure for keeping the borehole wall stable is well obtained by the three criteria, and borehole failure will basically not occur under this condition.

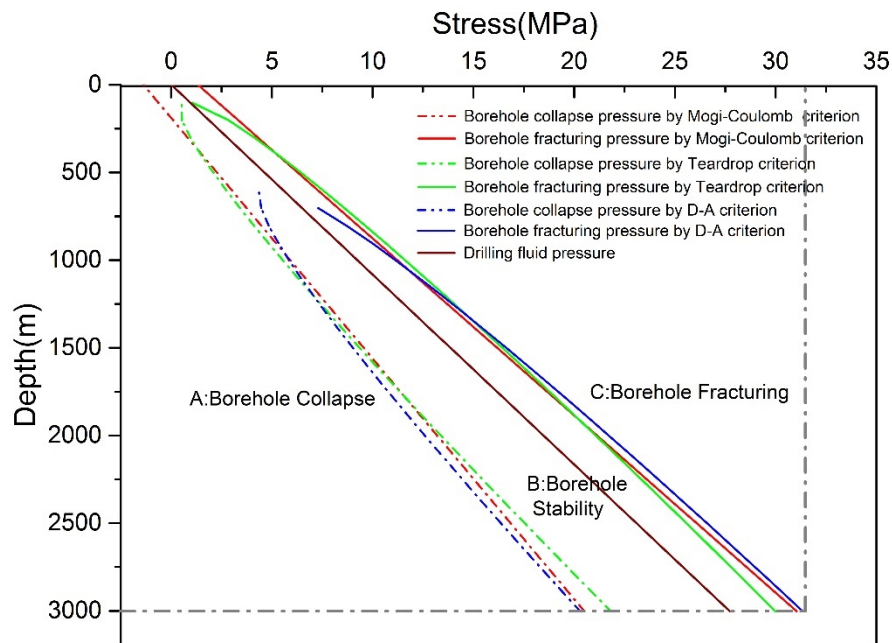


Figure 4. Critical borehole fracturing and collapse pressure considering the three failure criteria.

3.1.2. Study B: Influence of a Horizontal Stress Differential on Critical Borehole Fracturing and Collapse Pressure Considering Three Failure Criteria

When studying the in situ stress distribution, the horizontal stress differential coefficient d_c ($d_c = (\sigma_H - \sigma_h) / \sigma_h$) is often used to represent the difference in the layer internal stress. In study A, $\sigma_H = 8.8$ kPa/m and $\sigma_h = 8.5$ kPa/m, with $d_c = 0.0353$, so the situation indicates a very small horizontal stress difference. Nevertheless, we would meet high ice flow areas when drilling ice cores, and these areas mean a relatively larger horizontal stress difference. We take $\sigma_H = 8.5$ kPa/m and $\sigma_h = 7$ kPa/m, with $d_c = 0.2143$, to discuss the influence of ice horizontal pressure variation on critical borehole fracturing and collapse pressure between the three failure criteria (other parameter values are the same as Study A).

Figure 5 shows that with the critical pressure that is calculated by three failure criteria, these critical pressures maintain consistent trends with Study A. The safety drilling fluid pressure window becomes very narrow for the teardrop criterion. The most obvious change is that all critical pressures decrease greatly with an increase of d_c from 0.0353 to 0.2143. We can see that, when the depth exceeds 1000 m, the drilling fluid pressure is greater than any critical borehole pressure, which means an unavoidable borehole wall fracturing. This may be the reason for the phenomenon described in the study of Chen [24]. In a word, high ice flow speed (big horizontal stress differential) increases borehole instability.

3.1.3. Study C: Influence of Temperature and Strain Rate on Critical Borehole Fracturing and Collapse Pressure

1. The influence of temperature

The pressure phase transition, b_0 , the long axis of the ellipse, p_{sc} , and the tensile strength, σ_t , will change with the ice temperature. As a result, the critical value of the borehole fracturing and

collapse pressure (calculated by the teardrop and Derradji-Aouat criteria) will change accordingly. In order to study a variation trend that is caused by temperature, we take $-10\text{ }^{\circ}\text{C}$, $-15\text{ }^{\circ}\text{C}$, and $-20\text{ }^{\circ}\text{C}$ for discussion, and the other parameters are the same as in Study A above.

Figure 6 shows the critical pressure changes with temperature, as calculated by the teardrop criterion. The safety drilling fluid pressure window becomes broader with the decrease of temperature. The lower critical borehole collapse pressure and higher fracturing pressure indicate that ice behaves tougher at the temperature of $-20\text{ }^{\circ}\text{C}$, which means a more stable state of the borehole wall.

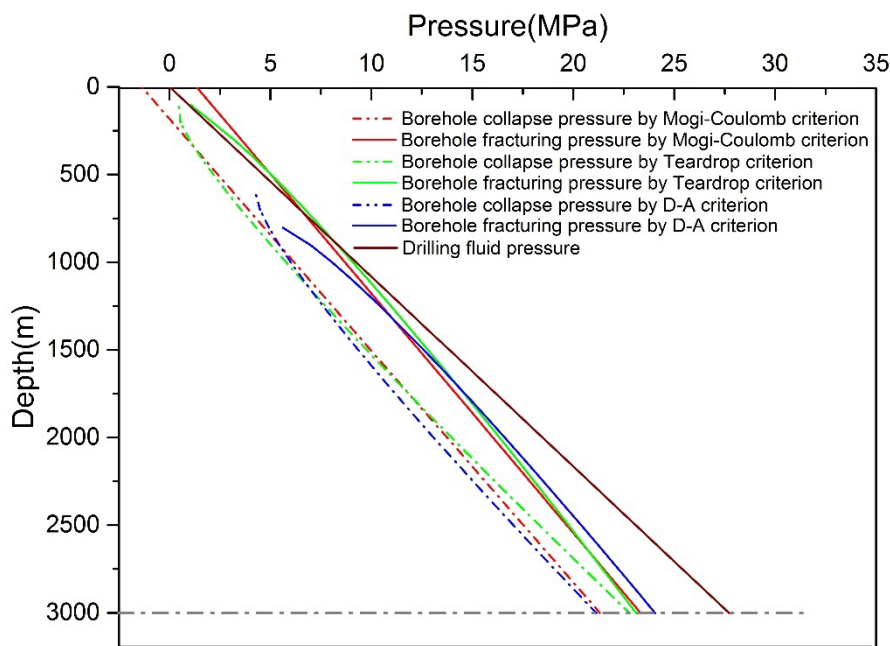


Figure 5. Critical borehole fracturing and collapse pressure considering three failure criteria ($d_c = 0.823$).

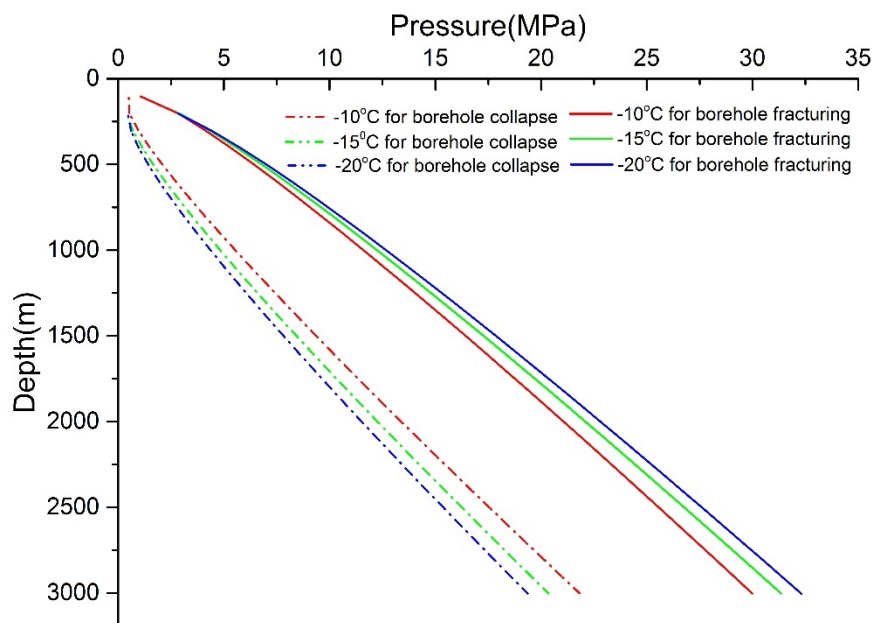


Figure 6. Critical borehole fracturing and collapse pressure changes at different temperatures calculated by the teardrop criterion.

However, the situation changes when using the Derradji-Aouat criterion for calculation (Figure 7). We can obtain certain critical pressures at shallow depths (less than $\sim 600\text{ m}$) by solving Equation (26)

at lower temperatures; the curves of the temperatures at $-15\text{ }^{\circ}\text{C}$ and $-20\text{ }^{\circ}\text{C}$ show crosscurrents compared to Figure 6, and the safety drilling fluid pressure window becomes broader with the increase of temperature. However, this rule is not in keeping with the curve at $-10\text{ }^{\circ}\text{C}$. We should notice that in this criterion, the strain rate is introduced for calculation, and this parameter may dominate this inconsonant phenomenon. Ice compression experiments have shown that at different temperatures, ice starts to become brittle at different loading strain rates [36–38], and the interaction between strain rate and temperature causes this non-uniform trend.

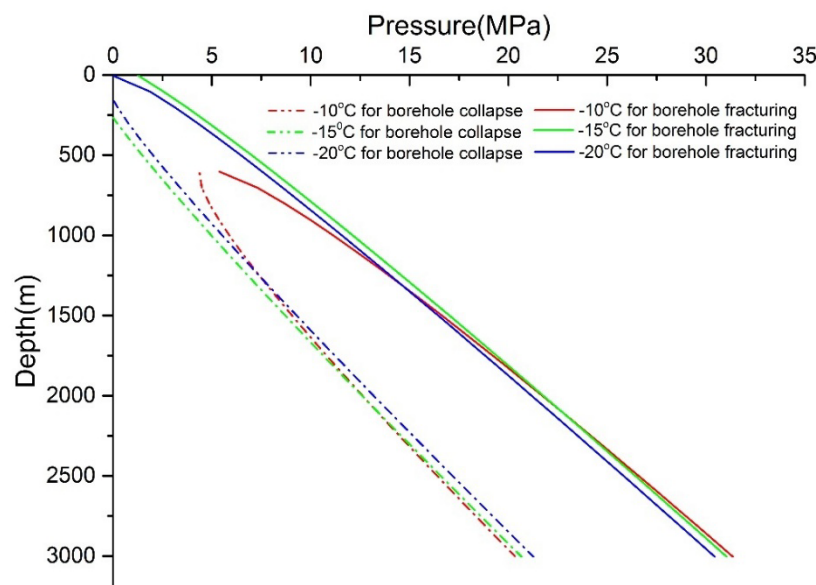


Figure 7. Critical borehole fracturing and collapse pressure changes at different temperatures, as calculated by the Derradji-Aouat criterion.

2. The Influence of Strain Rate

The parameter of strain rate has an important influence on the brittle fracture of ice (strain rate $\geq 10^{-3}$); ice behaves with different ultimate strengths at different loading strain rates [36–38]. As a result, the strain rate should also play an important role in determining the critical pressure in the ice borehole wall, which is contained in the Derradji-Aouat criterion. We chose a strain rate from 10^{-4} to 10^{-3} (ice ductile-to-brittle transition) to study the critical pressure changes as calculated by the Derradji-Aouat criterion.

From Figure 8, we can see that the safety drilling fluid pressure window becomes broader with the increase of the strain rate. In other words, a sudden brittle failure (higher strain rate) on the borehole wall requires a bigger pressure differential between the ice pressure and the drilling fluid pressure. In an actual ice borehole, we define borehole wall brittle failure under the conditions of strain rates $\geq 10^{-3}$ for borehole collapse and fracturing. Nonetheless, the deficiencies are that no real roots could be obtained by using the Derradji-Aouat criterion before $\sim 600\text{ m}$ at this temperature ($-10\text{ }^{\circ}\text{C}$), and further studies on the Derradji-Aouat criterion are needed for finding reasonable explanations for this.

3.2. Critical Pressure for a Fissured Ice Borehole Wall

The fissured ice borehole wall means that the wall contains small cracks where the drilling fluid can penetrate, which could reduce the stability of the borehole. On the basis of the theory discussed in Section 2.3, for certain ice stress states, a small crack length $2l_0$, a friction coefficient between cracks μ_c , and ice fracture toughness K_{IC} play important roles in determining the critical pressure for the fissured ice borehole wall.

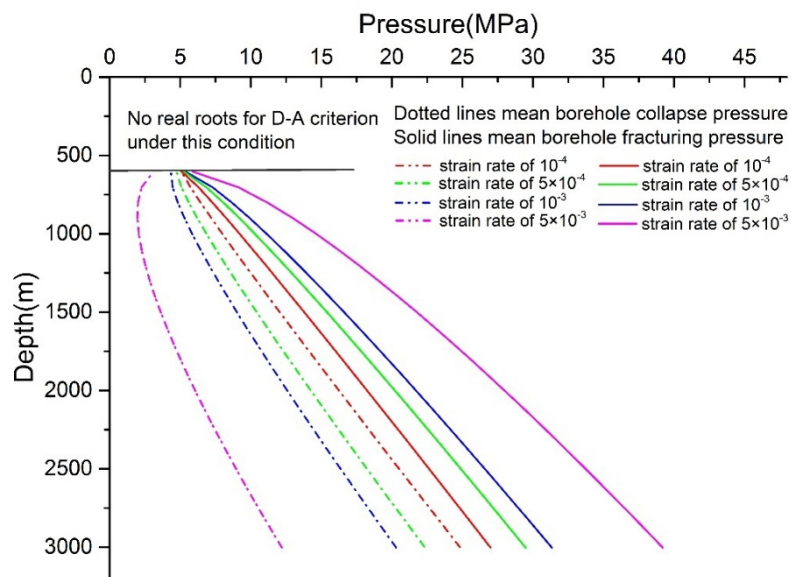


Figure 8. Critical borehole fracturing and collapse pressure changes at different strain rates calculated by the Derradji-Aouat criterion.

For the friction coefficient between cracks, take the lubrication of drilling fluid into consideration, and, according to Kennedy, Montagnat, and Schulson's tests result of fresh water granular ice sliding across itself on a smooth interface, with ice fracture under higher speeds, we accept the values of 0.1–0.2 [39–42]. As for the ice fracture toughness, a review of experiments conducted on ice is given by Schulson and Duval [38], and these results suggest a range of 0.1–0.4 MPa·m^{1/2}. We assume that the half-length of crack l_0 on the fissured ice borehole wall is 0.01–0.1 m, and other parameters are the same as in Study A, with a depth of 3000 m, for example. Figure 9 shows the critical pressure changes for borehole wall failure.

Comparing the curves in Figure 9, it is clear that:

1. For borehole collapse, the critical pressure decreases with an increase of the friction coefficient; a higher value of ice fracturing toughness and a longer fracture length on the borehole wall need a higher collapse pressure for borehole stability. The factor of the friction coefficient has the biggest impact on the results.
2. For borehole fracturing, the variation trend of the critical pressure is contrary to the collapse pressure, and the pressure increases with a higher friction coefficient, a higher ice fracture toughness, and a shorter fracture length. Similarly, the factor of the friction coefficient exerts a tremendous influence on the critical pressure.

In general, a smaller value of ice fracture toughness, a longer fracture length, and a lower friction coefficient reduce the stability of the borehole for the fissured ice borehole wall. The most important factor of the ice friction coefficient needs to be pinpointed when determining the safety pressure window in actual ice drilling.

In order to study the critical safety pressure window reduction due to ice borehole wall cracks, we compare all curves in Figure 10. All parameters are the same as in Study A for an unbroken wall. As for a fissured borehole wall, a friction coefficient of 0.1, a half crack length of 0.1 m, and an ice fracture toughness of 0.1 MPa·m^{1/2} are chosen to demonstrate the decrease to the utmost extent. We can see from Figure 10 that the borehole stable interval decreases a lot. Taking the borehole collapse and fracturing pressures calculated by the teardrop criterion at 3000 m for an example, the safety pressure window is 21.8–30.0 MPa, compared with 24.0–27.7 MPa for a fissured borehole wall, meaning that the borehole stable interval is reduced by 55%. According to these results, when we drill through a broken

zone of the ice layer, special concerns about the drilling fluid pressure (drilling fluid density) should be taken to avoid borehole failure for safety ice drilling.

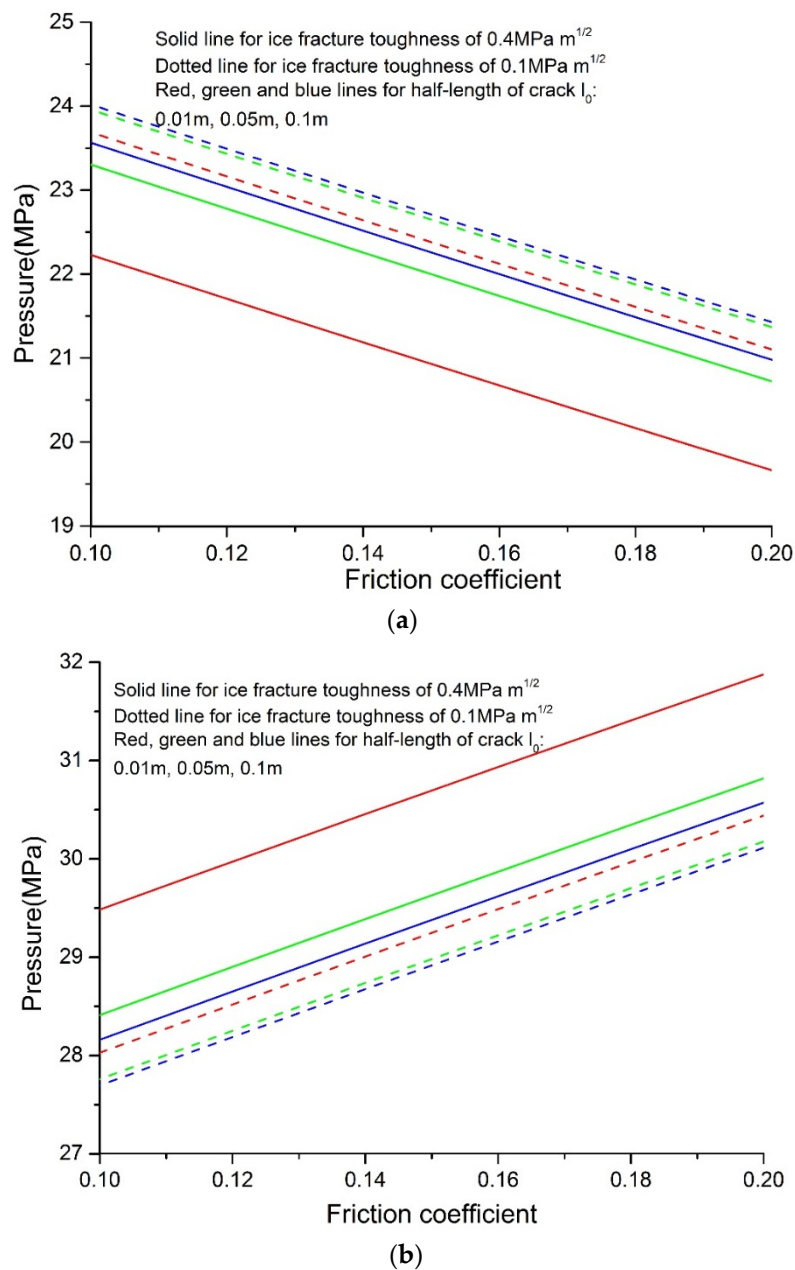


Figure 9. Critical borehole pressure changes for a fissured ice borehole wall at depth of 3000 m. (a) Borehole collapse; (b) borehole fracturing.

3.3. Discussion on Practical Applications and Suggestions

Through all circumstances above, it is clear that the main discussion of this method focuses on the brittle failure on a vertical borehole wall for an unbroken borehole wall. Nevertheless, we should notice that ice behaves in a ductile manner at a low strain rate ($<10^{-4}/\text{s}$), which refers to the ice creep. In actual ice drilling, even if we choose a reasonable drilling fluid density and control the borehole pressure through the method that we proposed above, there will still be a small pressure difference on the borehole wall. When considering the cumulative effect of time, ductile deformation could occur, due to this ice creep. Relevant research about borehole ductile deformation will be further studied. Meanwhile, we should point out that all conclusions are applied on a vertical borehole, which is the

form of almost all ice boreholes in polar regions. As for a fissured borehole wall, this theory focuses on the small closed crack on the borehole wall, and we ignore the crack extension on relatively large fractured zones. Besides, the effect of multiple cracks on the borehole wall has not yet been considered in this paper. We believe that these cracks will further weaken the borehole wall. Related studies will be carried out, following this paper.

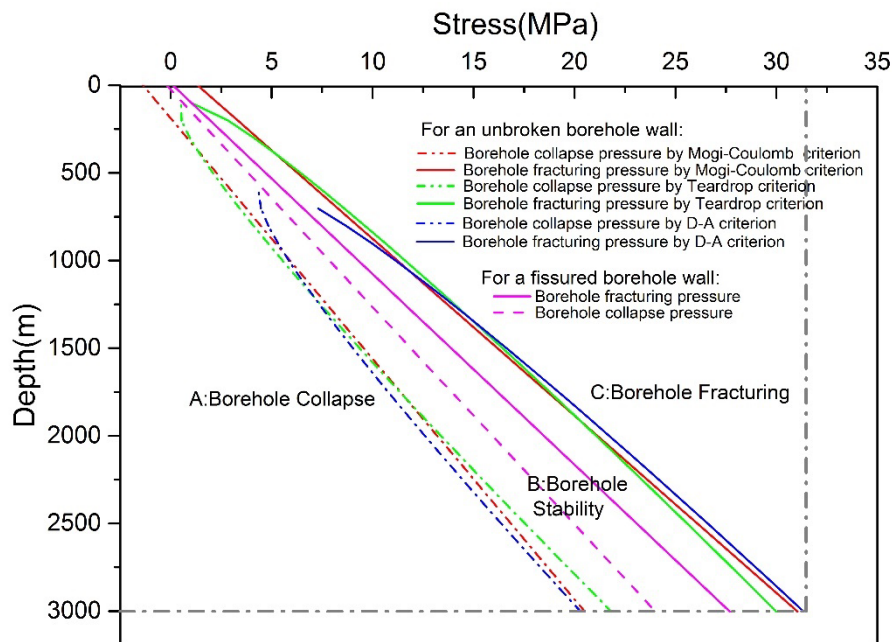


Figure 10. Comparison of the critical borehole pressure changes between an unbroken borehole wall and a fissured borehole wall.

According to the presented method, we are trying to tease out the specific application steps, to obtain the safety drilling fluid pressure window when drilling into ice sheets or glaciers. The first thing to consider is the determination of the state of the borehole wall. We can ensure the state through ice-core integrity (Figure 11). When the borehole wall is unbroken, the temperature variation in the borehole, the ice pressure distribution, and the strain rate (usually 10^{-3} /s for brittle failure) are obtained by actual measurements and are used to obtain a safety drilling fluid pressure window. Under this circumstance, we can obtain an adjust the drilling fluid density to keep the appropriate column pressure. As for a fissured borehole wall, the related implementation issues change by obtaining the friction coefficient (the most important factor compared to ice fracture toughness and crack/fracture length) in this condition. Following this line of thought, we can also obtain the corresponding pressure window and the relevant measures to adjust the drilling fluid density similarly.



Figure 11. Different ice-core states. (a) For an unbroken ice-core; (b) for a fissured ice-core.

4. Conclusions

This paper proposes a detailed method to ensure the maintenance of the safety drilling fluid pressure window in ice drilling boreholes. The theoretical results showed that:

1. For an unbroken borehole wall, no borehole collapse or fracturing occurred under the common drilling fluid pressure. At the same time, an analysis of factors influencing the borehole stability showed that: (1) a larger horizontal stress differential would increase the borehole instability. When drilling in high ice flow areas on ice sheets or glaciers, necessary measures of reducing the drilling fluid density should be taken to keep the borehole stable; (2) The effect of the strain rate on borehole stability showed that the safety drilling fluid pressure window became wider with the increase of the strain rate on the borehole wall, under the Derradji-Aouat criterion. When comparing such a window with the results calculated by the other two criteria, an approximate result came up at a strain rate of around 10^{-3} /s. (3) As for the temperature, such a window as calculated by Derradji-Aouat can show an interaction between the strain rate and the temperature better than the teardrop criterion.
2. For a fissured borehole wall, the ice friction coefficient played the most important role in determining the borehole critical failure pressure, compared with the factors of fracture toughness and fracture length. The borehole became more stable under the condition of shorter fracture length and higher friction coefficient and fracture toughness. At the same time, a maximum reduction of about 55% of the safety drilling fluid pressure window was calculated when comparing the fissured borehole wall to the unbroken one. In the actual application, we should pay more attention to the state of the ice core's integrity. If we drilled into a fissured ice layer, the necessary measures of adjusting the drilling fluid density should be taken, to ensure that the borehole pressure is within the calculated safety pressure window.

Author Contributions: H.Z. conceived and wrote the paper; D.P. and L.Z. analyzed the data; Y.Z. contributed analysis tools; C.C. proposed the theory.

Funding: This study was supported by the Chinese National Natural Science Foundation (No. 41876218 and No. 41672361), the Ministry of Land and Resources of China (No. 201311041), the Provincial and School Co-construction project (No. SXGJSF2017-5), and the Program for JLU Science and Technology Innovative Research Team (No. 2017TD-24).

Acknowledgments: The authors also thank Pavel Talalay and anonymous reviewers for fruitful discussion and useful comments.

Conflicts of Interest: The authors declare no conflicts of interest.

References

1. Chen, X.; Tan, C.P.; Detournay, C. A study on wellbore stability in fractured rock masses with impact of mud infiltration. *J. Pet. Sci. Eng.* **2003**, *38*, 145–154. [[CrossRef](#)]
2. Hashemi, S.S.; Taheri, A.; Melkoumian, N. Shear failure analysis of a shallow depth unsupported borehole drilled through poorly cemented granular rock. *Eng. Geol.* **2014**, *183*, 39–52. [[CrossRef](#)]
3. Lee, H.; Ong, S.H.; Azeemuddin, M.; Goodman, H. A wellbore stability model for formations with anisotropic rock strengths. *J. Pet. Sci. Eng.* **2012**, *96–97*, 109–119. [[CrossRef](#)]
4. Gholami, R.; Moradzadeh, A.; Rasouli, V.; Hanachi, J. Practical application of failure criteria in determining safe mud weight windows in drilling operations. *J. Rock Mech. Geotech. Eng.* **2014**, *6*, 13–25. [[CrossRef](#)]
5. Al-Ajmi, A.M.; Zimmerman, R.W. Stability analysis of vertical boreholes using the Mogi–Coulomb failure criterion. *Int. J. Rock Mech. Min.* **2006**, *43*, 1200–1211. [[CrossRef](#)]
6. Hobbs, D.W. The Strength and the Stress-Strain Characteristics of Coal in Triaxial Compression. *J. Geol.* **1964**, *72*, 214–231. [[CrossRef](#)]
7. Handin, J.; Heard, H.C.; Magouirk, J.N. Effects of the intermediate principal stress on the failure of limestone, dolomite, and glass at different temperatures and strain rates. *J. Geophys. Res.* **1967**, *72*, 611–640. [[CrossRef](#)]

8. Mogi, K. Fracture and Flow of Rocks under High Triaxial Compression. *J. Geophys. Res.* **1971**, *76*, 1255–1269. [[CrossRef](#)]
9. Hoek, E.; Brown, E.T. Practical estimates of rock mass strength. *Int. J. Rock Mech. Min.* **1997**, *34*, 1165–1186. [[CrossRef](#)]
10. Franklin, J.A. Triaxial strength of rock materials. *Rock Mech.* **1971**, *3*, 86–98. [[CrossRef](#)]
11. Colmenares, L.B.; Zoback, M.D. A statistical evaluation of intact rock failure criteria constrained by polyaxial test data for five different rocks. *Int. J. Rock Mech. Min.* **2002**, *39*, 695–729. [[CrossRef](#)]
12. Haimson, B.C.; Chang, C.D. True triaxial strength of the KTB amphibolite under borehole wall conditions and its use to estimate the maximum horizontal in situ stress. *J. Geophys. Res.* **2002**, *107*, ETG 15-11–ETG 15-14. [[CrossRef](#)]
13. Aadnoy, B.S.; Froitland, T.S. Stability of adjacent boreholes. *J. Pet. Sci. Eng.* **1991**, *6*, 37–43. [[CrossRef](#)]
14. Fuh, G.F.; Whitfill, D.L.; Schuh, P.R. Use of borehole stability analysis for successful drilling of high-angle hole. In Proceedings of the IADC/SPE Drilling Conference, Dallas, TX, USA, 28 February–2 March 1988.
15. McLean, M.R.; Addis, M.A. Wellbore stability: The effect of strength criteria on mud weight recommendations. In Proceedings of the 65th Annual Technical Conference and Exhibition of SPE, New Orleans, LA, USA, 23–26 September 1990.
16. Al-Ajmi, A.M.; Zimmerman, R.W. Relation between the Mogi and the Coulomb failure criteria. *Int. J. Rock Mech. Min.* **2005**, *42*, 431–439. [[CrossRef](#)]
17. Vernik, L.; Zoback, M.D. Strength anisotropy in crystalline rock: Implications for assessment of in situ stresses from wellbore breakouts. In Proceedings of the 31st US Symposium on Rock Mechanics Contributions and Challenges, Rotterdam, The Netherlands, 18–20 June 1990.
18. Liang, C.; Chen, M.; Jin, Y.; Lu, Y.H. Wellbore stability model for shale gas reservoir considering the coupling of multi-weakness planes and porous flow. *J. Nat. Gas Sci. Eng.* **2014**, *21*, 364–378. [[CrossRef](#)]
19. Ma, T.S.; Chen, P. A wellbore stability analysis model with chemical-mechanical coupling for shale gas reservoirs. *J. Nat. Gas Sci. Eng.* **2015**, *26*, 72–98. [[CrossRef](#)]
20. Karatela, E.; Taheri, A.; Xu, C.S.; Stevenson, G. Study on effect of in-situ stress ratio and discontinuities orientation on borehole stability in heavily fractured rocks using discrete element method. *J. Petrol. Sci. Eng.* **2016**, *139*, 94–103. [[CrossRef](#)]
21. Talalay, P.; Fan, X.P.; Xu, H.W.; Yu, D.H.; Han, L.L.; Han, J.J.; Sun, Y.H. Drilling fluid technology in ice sheets: Hydrostatic pressure and borehole closure considerations. *Cold Reg. Sci. Technol.* **2014**, *98*, 47–54. [[CrossRef](#)]
22. Fujii, Y.; Azuma, N.; Tanaka, Y.; Nakayama, Y.; Kameda, T.; Shinbori, K.; Katagiri, K.; Fujita, S.; Takahashi, A.; Kawada, K. Deep ice core drilling to 2503 m depth at Dome Fuji, Antarctica. *Mem. Natl. Inst. Polar Res. Spec. Issue* **2002**, *56*, 103–116.
23. Lyle, H.B.; Gundestrup, N.S. Resurvey of Bore Hole at Dye 3, South Greenland. *J. Glaciol.* **2017**, *34*, 178–182. [[CrossRef](#)]
24. Chen, C.; Zhang, H.; Liu, S.Y.; Jin, C.C.; Chen, Y.; Zhang, N. Hydraulic fracturing in ice boreholes: Theory and tests. *Polar Sci.* **2018**, in press. [[CrossRef](#)]
25. Nadreau, J.P.; Nawwar, A.M.; Wang, Y.S. Triaxial testing of freshwater ice at low confining pressures. *J. Offshore Mech. Arct.* **1991**, *113*, 260–265. [[CrossRef](#)]
26. Derradji-Aouat, A. Multi-surface failure criterion for saline ice in the brittle regime. *Cold Reg. Sci. Technol.* **2003**, *36*, 47–70. [[CrossRef](#)]
27. Westergaard, H.M. Plastic state of stress around a deep well. *J. Boston Soc. Civ. Eng.* **1940**, *27*, 1–5.
28. Gnirk, P.F. The Mechanical Behavior of Uncased Wellbores Situated in Elastic/Plastic Media under Hydrostatic Stress. *Soc. Pet. Eng. J.* **1972**, *12*, 49–59. [[CrossRef](#)]
29. Mitchell, R.F.; Goodman, M.A.; Wood, E.T. Borehole stresses: Plasticity and the drilled hole effect. In Proceedings of the IADC/SPE Drilling Conference, New Orleans, LA, USA, 15–18 March 1987.
30. Anthony, J.L.; Crook, J.Y. Development of an orthotropic 3D elastoplastic material model for shale. In Proceedings of the SPE/ISRM Rock Mechanics Conference, Irving, TX, USA, 20–23 October 2002.
31. Ashby, M.F.; Hallam, S.D. The failure of brittle solids containing small cracks under compressive stress states. *Acta Metall.* **1986**, *34*, 497–510. [[CrossRef](#)]
32. Lin, P. Brittle Failure Behavior of Media Containing Cracks and Holes. Ph.D. Thesis, Northeastern University, Shenyang, China, 2 February 2002.

33. Zhen, G. Research on the Damage and Fracture Mechanism of Wellbore Stability. Ph.D. Thesis, Harbin Engineering University, Harbin, China, 20 May 2005.
34. Hooke, R.L. *Principles of Glacier Mechanics*, 2nd ed.; Cambridge University Press: Cambridge, UK, 2005.
35. Shan, R.; Bai, Y.; Huang, P.; Song, Y.; Guo, X. Experimental Research on Failure Criteria of Freshwater Ice under Triaxial Compressive Stress. *Chin. J. Theor. Appl. Mech.* **2017**, *49*, 467–477.
36. Rist, M.A.; Murrell, S.A.F. Ice triaxial deformation and fracture. *J. Glaciol.* **1994**, *40*, 305–318. [[CrossRef](#)]
37. Gagnon, R.E.; Gammon, P.H. Triaxial experiments on iceberg and glacier ice. *J. Glaciol.* **1995**, *41*, 528–540. [[CrossRef](#)]
38. Duval, P. *Creep and Fracture of Ice*; Cambridge University Press: Cambridge, UK, 2009.
39. Beeman, M.; Durham, W.B.; Kirby, S.H. Friction of ice. *J. Geophys. Res. Solid Earth* **1988**, *93*, 7625–7633. [[CrossRef](#)]
40. Montagnat, M.; Schulson, E.M. On friction and surface cracking during sliding of ice on ice. *J. Glaciol.* **2003**, *49*, 391–396. [[CrossRef](#)]
41. Kietzig, A.M.; Hatzikiriakos, S.G.; Englezos, P. Physics of ice friction. *J. Appl. Phys.* **2010**, *107*, 4. [[CrossRef](#)]
42. Schulson, E.M.; Fortt, A.L.; Iliescu, D.; Renshaw, C.E. On the role of frictional sliding in the compressive fracture of ice and granite: Terminal vs. post-terminal failure. *Acta Mater.* **2006**, *54*, 3923–3932. [[CrossRef](#)]



© 2018 by the authors. Licensee MDPI, Basel, Switzerland. This article is an open access article distributed under the terms and conditions of the Creative Commons Attribution (CC BY) license (<http://creativecommons.org/licenses/by/4.0/>).